PRACA ORYGINALNA

Computer aided subthalamic nucleus (STN) localization during deep brain stimulation (DBS) surgery in Parkinson's patients

Komputerowo wspomagana lokalizacja jądra niskowzgórzowego (STN) w przebiegu operacji głębokiej stymulacji mózgu (DBS) u pacjentów z chorobą Parkinsona

Konrad Ciecierski[1], Tomasz Mandat[2,3], Rafał Rola[4], Zbigniew W. Raś[5,1], Andrzej W. Przybyszewski[6,7]

Received: 20.06.2014
Revised: 25.08.2014
Accepted: 08.09.2014
Published online: 12.11.2014

:

ABSTRACT

INTRODUCTION

During deep brain stimulation (DBS) treatment of Parkinson's disease, the anatomical target of the surgery is a small (9 x 7 x 4 mm) deeply located structure called the Subthalamic Nucleus (STN). It is similar morphologically to the surrounding tissue and as such, not easily distinguished in CT or MRI. The goal of the surgery is precise placement of a permanent stimulating electrode within the target nucleus. Precision is extremely important as incorrect placement of the stimulating electrode may lead to serious adverse effects such as mood disturbances.

MATERIALS AND METHODS

To obtain the exact location of the STN nucleus, intraoperative stereotactic supportive navigation is used. A set of 3 ~ 5 parallel microelectrodes is inserted into the brain and advanced towards the expected location of the nucleus. From a depth of 10 mm above the estimated STN, the electrodes advance at 1 mm steps. At each step, the activity of the surrounding neural tissue is recorded. Typically, the electrodes are further advanced until the ventral STN border is passed and the Substantia Nigra pars reticulata (SNr) is reached.
Because the STN has distinct physiological properties, signals recorded in the vicinity of the STN display specific features. Therefore it was possible to provide an analytical method to detect specific STN characteristics. This paper presents a computer-based approach in order to discriminate between microelectrode signals coming from the STN and those outside it.

RESULTS AND CONCLUSIONS

When our method was used on-line during DBS neurosurgical procedure, it helped in precise identification of STN borders and shorted the surgery. Since

[1]Warsaw University of Technology, Institute of Computer Science in Warsaw
[2]Department of Neurosurgery, Institute of Oncology in Warsaw
[3]Department of Neurosurgery, Institute of Psychiatry and Neurology in Warsaw
[4]1st Department of Neurology, Institute of Psychiatry and Neurology in Warsaw
[5]University of North Carolina, Department of Computer Science, Charlotte, NC 28223, USA
[6]UMass Medical School, Department of Neurology, Worcester, MA 01655, USA
[7]Polish-Japanese Institute of Information Technology in Warsaw

ADRES DO KORESPONDENCJI:

Dr inż. Konrad Ciecierski
Wydział Elektroniki i Technik Informacyjnych
Politechnika Warszawska
ul. Nowowiejska 15/19
00-665 Warszawa
e-mail: k.ciecierski@ii.pw.edu.pl

Ann. Acad. Med. Siles. 2014, 68, 5, 275–283

eISSN 1734-025X
www.annales.sum.edu.pl

the fall of 2013, we have developed an on-line computer-aided application for STN border localization that is used during PD DBS surgeries performed in the Institute of Psychiatry and Neurology in Warsaw, POLAND.

KEY WORDS
Parkinson's disease, DBS, STN, Spike detection, Spike sorting, Wavelet, Neuronal noise, Signal power

STRESZCZENIE

WSTĘP

Podczas zabiegu głębokiej stymulacji mózgu (*deep brain stimulation* – DBS) stosowanego w leczeniu choroby Parkinsona celem operacji jest mała (9 x 7 x 4 mm) głęboko położona struktura mózgu nazywana jądrem niskowzgórzowym (*subthalamic nucleus* – STN). Struktura ta jest morfologicznie podobna do otaczających ją tkanek i jako taka niezbyt dobrze rozróżnialna w obrazowaniu tomografem komputerowym (CT) lub rezonansem magnetycznym (MRI). Celem zabiegu operacyjnego jest precyzyjna implantacja stymulującej elektrody w docelowym jądrze. Precyzja jest niesłychanie istotna, ponieważ niewłaściwe umiejscowienie stymulującej elektrody może doprowadzić do wystąpienia poważnych efektów ubocznych, takich jak zaburzenia nastroju.

MATERIAŁ I METODY

Aby uzyskać dokładne położenie STN w trakcie operacji, używana jest wspomagająca nawigacja stereotaktyczna. Zestaw 3~5 równoległych elektrod jest wprowadzany do mózgu pacjenta i zagłębiany w kierunku spodziewanej lokalizacji STN. Od głębokości około 10 mm ponad spodziewanym STN elektrody są zagłębiane z krokiem 1 mm. Po każdym takim kroku rejestrowana jest aktywność tkanki nerwowej otaczającej elektrody. Najczęściej elektrody są dalej zagłębiane, aż przekroczą dolną granicę STN i osiągną istotę czarną część siatkowatą (*substantia nigra pars reticulata* – SNr). Ponieważ STN przejawia specyficzne właściwości fizjologiczne, sygnały zarejestrowane w jego okolicy również mają wyróżniające właściwości. Można przez to stworzyć analityczne metody wykrywające te specyficzne dla STN właściwości. W niniejszej publikacji zaprezentowano podejście informatyczne, pozwalające na wykrywanie zarejestrowanych sygnałów pochodzących z wewnątrz oraz spoza STN.

WYNIKI I WNIOSKI

Zastosowanie naszej metody w trakcie zabiegów operacyjnych pomogło w precyzyjnej lokalizacji granic STN oraz pozwoliło skrócić czas zabiegu. Od jesieni 2013 opracowujemy aplikację do wspomagania lokalizacji STN, która jest używana w trakcie zabiegów DBS przeprowadzanych w leczeniu choroby Parkinsona w Instytucie Psychiatrii i Neurologii w Warszawie.

SŁOWA KLUCZOWE
choroba Parkinsona, DBS, STN, wykrywanie potencjałów czynnościowych, grupowanie potencjałów czynnościowych, falki, neuronowy szum tła, moc sygnału

INTRODUCTION

Parkinson's disease (PD) is a chronic and progressive movement disorder. The risk factor of the disease increases with the age. As the average human life span elongates, the number of people affected with PD also steadily increases. Because of the nature of the illness – affecting the patient's movement without impairment of his intelligence and/or consciousness – it has a very high social cost. People as early as in their 40s, otherwise fully functional are seriously disabled and require constant additional external support. According to current medical knowledge, PD is caused by low levels of a chemical component called dopamine [1,2]. Dopamine is produced by specific cells in the brain region called the Substantia Nigra (SN). The main cause of PD is the process of dying of those cells. Its cause (and by this the cause of PD) is idiopathic. As the main causes of the disease are not clear, there cannot be an effective cure for them. The treatment focuses on symptoms of the disease. The main treatment for the disease is pharmacology. Pharmacotherapy provides the organism with a replacement

of the missing dopamine. Unfortunately, generally the effectiveness of the treatment decreases with time. In such cases, after fulfilling certain medical requirements [3] patients can be qualified for surgical treatment of PD.

This kind of surgery is called Deep Brain Stimulation (DBS). The goal of the surgery is placement of a permanent stimulating electrode into the STN. This nucleus is a small structure – placed deep within the brain that unfortunately does not show well in either CT or MRI scans. The stimulating electrode when properly placed disrupts the overactive neural circuits that are responsible for forming the rigidness typical for the advanced stage of Parkinson's Disease. Incorrect placement of the stimulating electrode might, however, evoke various serious adverse side effects. For example, placement of the electrode off by a few millimeters can cause severe emotional imbalance [4,5].

Having only a rough location of the STN, during DBS surgery precise localization of the STN has to be achieved by other means. Stereotactic navigation and intra-operative localization have to be introduced. A set of 3 ~ 5 parallel microelectrodes is inserted into the brain and advanced towards the expected location of the nucleus. From a depth of about 10 mm above the estimated STN center, the electrodes start to advance at 1 mm steps. At each step, the activity of the surrounding neural tissue is recorded. Typically, the electrodes are further advanced until the ventral STN border is passed and the Substantia Nigra pars reticulata (SNr) is reached [6,7].

As one of the hallmarks of PD is hyperactivity of the STN, this should be reflected in recordings coming from it [8]. By calculating specific attributes, one can discriminate between the recordings coming from the STN and those from structures adjacent to it. Those attributes, described in the next section, have been proven to constitute a foundation that is sufficient to create a computer classifier that discriminates the recordings from microelectrodes with sensitivity of 0.93 and specificity over 0.98.

Fast implementation of the attributes and classification calculation process allows the computer program to provide results in about two minutes. Such a fast calculation allows us to use this software during surgery in the operation theatre.

MATERIALS AND METHODS

Attributes that can be obtained from the microelectrode recorded signal can be most generally divided into two groups: based upon spike occurrence and neuronal background noise.

1. Attributes based on spike occurrence

Assuming that the recording has filtered out low frequencies and that the amplitude's moving average does not fluctuate, spikes can be detected based upon their high amplitude. One can assume that if the modulus of the amplitude at a certain time is greater than 4σ (see Section 5), then it might indicate the presence of a spike [9,10]. This condition although necessary, is not sufficient and additional constraints have to be met to find the proper spike occurrence. The spikes' shape is determined by ion channels in the axon hillock. While different neurons do produce spikes of different shape, all of those shapes must fit into a certain shape range [11].

Those constraints must be specified for spikes of both polarities observed in the recordings. As shown in Figure 1, the detected spike is assumed to begin 0.5 ms before its peak and lasts for 1.1 ms after it.

The areas in gray indicate the forbidden amplitude.

Spikes that cross the threshold of 4σ but do enter those areas are not considered. In this way highly distorted or overlapping spikes are discarded. As the shape of the spike that is registered by the electrode depends both on neuron morphology and its distance from the electrode, one can use it to distinguish between spikes coming from different neuron cells [12,13,14].

The amplitude values used in defining the forbidden amplitude areas are defined based on the 4σ indicated by the black horizontal line.

A high spiking rate and bursting characterize STN neural activity. Those features are the basis for defining the first two STN distinguishing attributes. The first attribute states the average number of spikes that were observed in a given recording. The second attribute, called *burst ratio* is based upon intra-spike intervals, it gives the percentage of them that are not longer than 33 ms.

After spike sorting, i.e. the process of grouping them by their shapes, it is also possible to calculate those two attributes for each neuron whose activity was observed during recording. Having done that, one can select the attribute maximum value and provide the average number of spikes per second and burst ratio for the most active observed cell.

2. Attributes based upon signal background

While an electrode can detect spikes from neurons that are within a 50 μm radius from the tip, it still detects the general neuronal noise produced by all the neurons in much larger vicinity. This background noise depends primarily on the number of neurons in the neighborhood of the electrode and their average activity. As the STN contains large amounts of small and

highly active neuron cells [1], the background noise observed in recordings taken from it is also noticeably larger than in the adjacent structures. This is especially evident when comparing recordings from the STN and SNr. As seen in Figure 2, both recordings contain a large amount of frequently occurring spikes. However, only the STN recording presents elevated background noise.

The voltages produced by neurons are very small. Being generally below the level of 5 mv [1], they have to be greatly amplified during the recording process. This amplification also causes great sensitivity to any external contamination. Such minuscule intrusions as touching the stereotactic frame, patient movement or speaking during the recording process creates high amplitude artifacts [1]. Those artifacts can be responsible for even a 100 fold increase in signal power and must be removed prior to the calculation of any background attributes. Those artifacts are most evident in frequencies below 375 Hz. Careful wavelet based analysis of the signal in this frequency band allows us to remove contaminated parts of the signal while retaining the artefact free parts of it. The effectiveness of this process can be seen in Figure 3. The whole process of artifact removal is fully automatic and unsupervised.

While spike detection is less sensitive to the degree of amplification of the recorded signal, the background noise attributes depend heavily on this factor. There is no guarantee that in each surgery the amplification is the same and that the electrical properties of the electrodes are absolutely constant. To take this

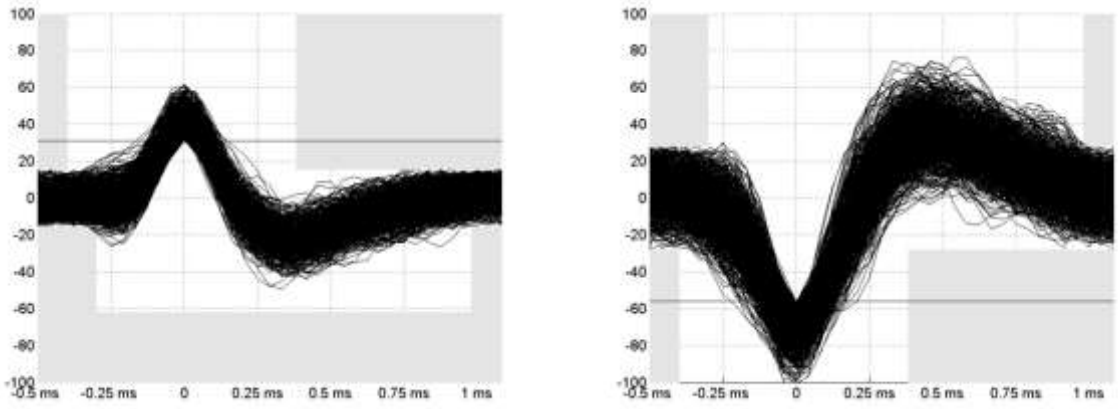

Fig. 1. Areas of forbidden amplitude for both polarities.
Ryc. 1. Obszary zakazane amplitudy dla obu polaryzacji.

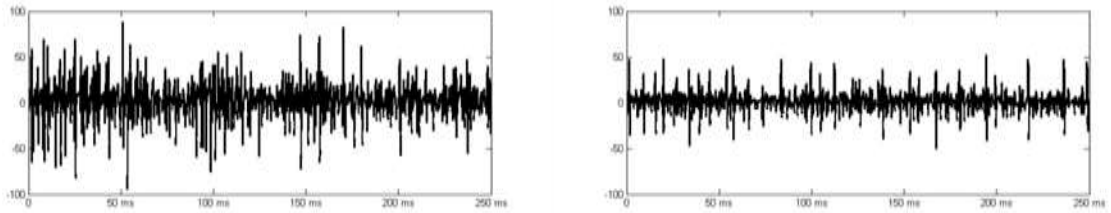

Fig. 2. 250 ms long recording fragments taken in STN (left) and SNr (right).
Ryc. 2. Długie fragmenty nagrań (250 ms) wykonanych w STN (z lewej) i SNR (z prawej)

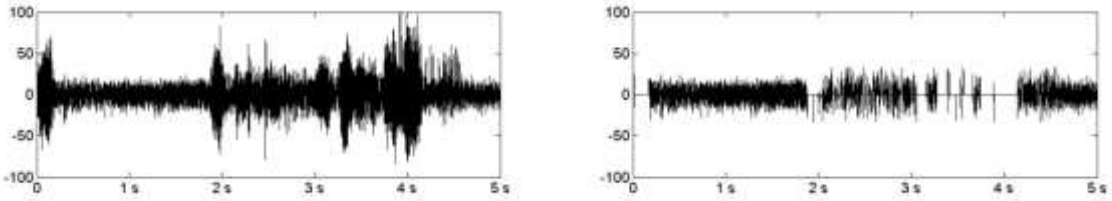

Fig. 3. 5s long highly contaminated signal before and after removal of the artifacts.
Ryc. 3. Fragmenty długości 5s- silnie zanieczyszczony sygnał przed i po usunięciu artefaktów.

into account some normalization has to be present. Without it, one could not safely compare the results taken from different electrodes and/or surgeries.

As stated in the introduction, the electrodes start their recording steps at the level of about 10 000 μm (10 mm) above the expected center of the STN. This implies that the first five recorded depths should be dorsal to the STN and be (with possible Thalamus traverse at around – 10 000 μm) recorded within white matter. The average value of any background attribute taken from those first five depths can be thus treated as the base normalizing value. From this, e.g. if for a selected electrode at a given depth an attribute has a value of 4, then it means that its value is four times larger than its average from the mentioned first five depths recorded by this electrode. This normalization is applied to all the described background attributes.

There are four primary background based attributes. The first attribute is based upon the amplitude percentile. When one is to consider the absolute values of the recorded signal amplitude, it is evident that all spiking activity occur after the 95th percentile. The lower percentile chosen, the smaller chance that it is influenced by any spike activity and that only the amplitude of the background noise is measured. A too low percentile will, however, start to also cut off also the background noise and the difference between STN and non-STN recordings will start to be less evident. Good results can be obtained using the 80th percentile since, it removes all spiking activity and retains background noise. This attribute is denoted as PRC_{80}.

The second background attribute is a standard Root Mean Square (RMS) calculated for the whole artifact free part of the signal. It takes into account both background noise and spiking activity.

The last two primary background attributes represent the signal power in selected frequency ranges. To calculate both attributes, besides prior removal of artifacts, all previously detected spikes are removed as well. This allows for calculation of the power only for the signal background. Without prior spike removal, the power is heavily influenced by the spike occurrence and (mentioned in spike-based attributes) false positive detections do occur.

The power is calculated using wavelets for frequency ranges 0−500 Hz for low frequency background power (LFB) and 500−3000 Hz for high frequency background power (HFB).

From the four primary background attributes four additional attributes are derived. Those attributes are the moving average of the primary attributes. The average for each depth is calculated from the value at this depth and two adjacent dorsal and ventral depths.

RESULTS

As described in Section 2.1, the first spike-based attribute states the average number of spikes that were observed in a given recording. When calculated for over 16 000 recordings, the quartiles for the recordings obtained from outside of the STN were

$$Q_1 = 0.000 \quad Q_2 = 0.000 \quad Q_3 = 6.889$$

And for the recordings obtained within the STN they were

$$Q_1 = 10.700 \quad Q_2 = 18.900 \quad Q_3 = 29.100$$

The second spike-based attribute, called *burst ratio* is based upon intra-spike intervals, it gives the percentage of them that are not longer than 33 ms. The quartiles for recordings obtained from outside of the STN were

$$Q_1 = 0.000 \quad Q_2 = 0.000 \quad Q_3 = 0.336$$

And for the recordings obtained within the STN they were

$$Q_1 = 0.416 \quad Q_2 = 0.580 \quad Q_3 = 0.711$$

While spike-based attributes provide non-overlapping Q_1~Q_3 ranges, they are not sufficiently good for discrimination between STN and non-STN recordings. They tend to produce both false positive and false negative results. False positives come from highly active non-STN neuron cells. Such high spiking activity can come for example from the *Thalamus* that is sometimes passed dorsally to the STN. False negatives might occur when the electrode recording lead happens to be in the less active parts of the STN.

In Figure 4 the values of the first two spike-based attributes calculated for a pass of three electrodes are shown. The electrodes recorded neural activity at depths from −10 000 μm up to +4000 μm with steps of 1000 μm (1 mm). The STN has been intraoperatively located by the Anterior and Medial electrodes on at depths ranging from −2000 to +2000 μm. The false positive results provided by the average number of spikes per seconds at depths −7000 and −6000 μm are clearly visible. Moreover, for the anterior electrode the high bursting ratio that can be seen at depth +4000 μm does not originate from within the STN.

Figure 5 (left) shows the values of the PRC_{80} attribute for the same electrode set that provided data for Figure 4. It is evident that this attribute provides much clearer detection of the STN and also there are no cases of falsely positive high values outside of the −2000 to +2000 area.

The Anterior and Medial electrodes did pass through the STN. The Central electrode entered the lateral part of the STN and only superficially passed through the nucleus. It was related to the differences between the

electrode track and anatomical coordinates of the STN. For the Anterior and Medial electrode, the 80th percentile of the amplitude registered within the STN was over twice as large as the referencing value calculated from the first five depths.

Figure 5 (right) shows the values of the RMS attribute for the same electrode set that provided data for Figures 4 and 5. Just as in the case of the PRC_{80}, this attribute also implies that the anterior electrode traversed the STN at depths –2000 to +2000 μm and that the Medial electrode traversed the STN at depths –2000 to +1000 μm (for the Medial electrode +2000 seems to indicate the ventral STN border).

The results obtained from the LFB and HFB attributes are consistent with the two previous background attributes. What is often observable is the brief decrease in LFB power inside of the STN. In this example, this decrease is evident at depth –1000 μm for the Anterior and Medial electrodes. It is also observable for the Central electrode at +2000 μm. This point of decreased power can be associated with the border between the adjacent STN territories [4,15].

Having defined the discriminating attributes, we were able to construct a classifier that when trained upon existing recordings it would be able to classify any new recording as to whether it had originated from within the STN or not [16,17,18].

Two classifiers were tested for this purpose. The first classifier is the Random Forest implementation provided by Weka v 3.7.9. Weka is a collection of machine learning algorithms written in Java and developed at the University of Waikato, New Zealand. (www.cs.waikato.ac.nz/ml/weka).

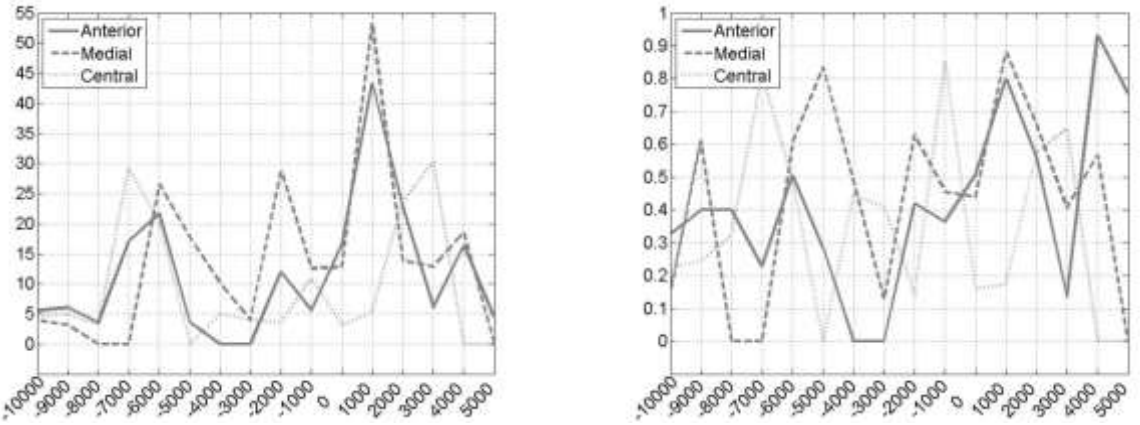

Fig. 4. Average number of spikes per second (left) and burst ratio (right).
Ryc. 4. Średnia liczba iglic na sekundę (z lewej) i współczynnik rozerwania (z prawej)

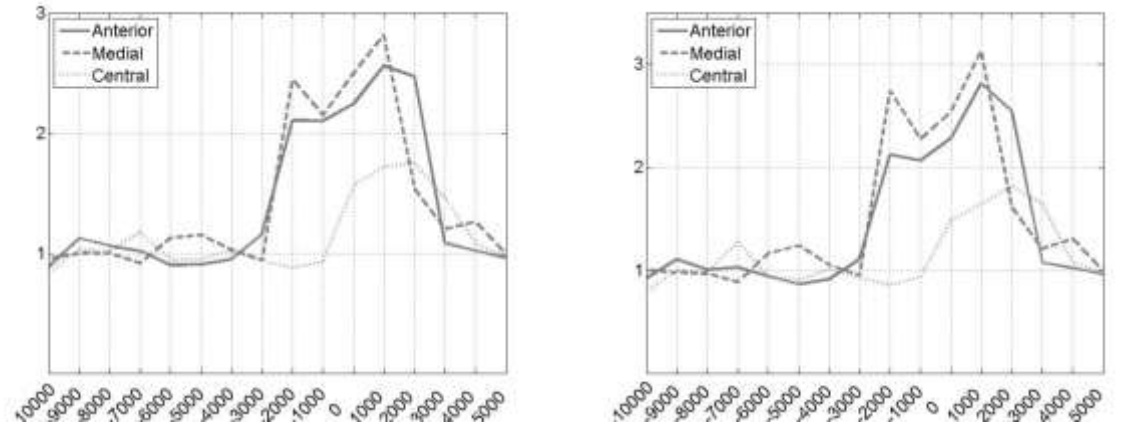

Fig. 5. Values of the PRC_{80} attribute (left) and RMS attribute (right).
Ryc. 5. Wartości atrybutu PRC_{80} (z lewej) i atrybutu RMS (po prawej)

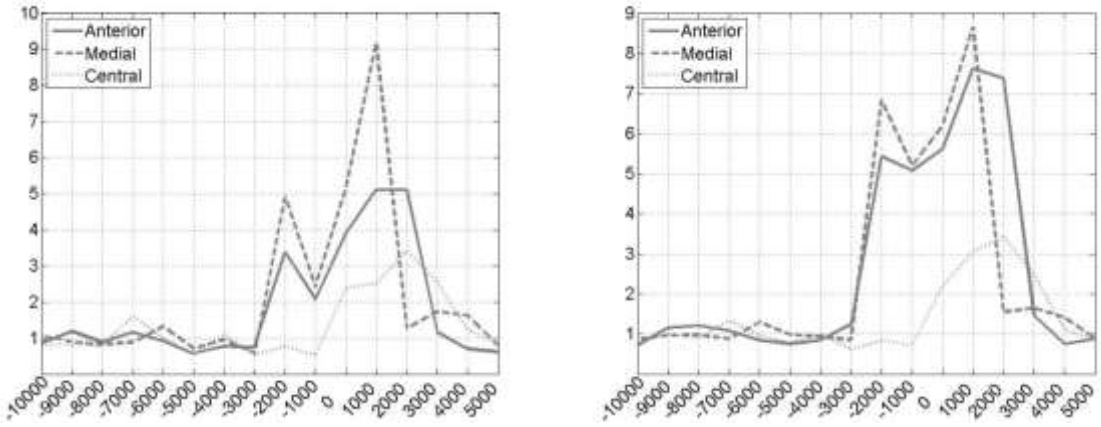

Fig. 6. Values of LFB (left) and HFB (right) attribute.
Ryc. 6. Wartości LFB (z lewej) i HFB atrybutu (z prawej).

The second classifier is provided by the RSES v 2.2.2 software. RSES builds the classifier using the rough set approach [19,20]. RSES stands for Rough Set Exploration System and is a software tool that provides the means for analysing tabular data sets using various methods – in particular those based on the Rough Set Theory.
(http://logic.mimuw.edu.pl/~rses/start.html)
Both classifiers were tested with the 10 fold cross validation method on 16 733 recordings.
In the case of spike-based attributes, the classifiers gave the following statistics:

Weka's Random Forest 10 fold cross validation:

Sensitivity:	0.476	Specificity:	0.909
Accuracy:	0.810	Coverage:	1.000

RSES 10 fold cross validation:

Sensitivity:	0.581	Specificity:	0.859
Accuracy:	0.796	Coverage:	0.976

Good specificity and poor sensitivity suggest that spike-based attributes, while good enough to detect recordings coming from outside of the STN, they are clearly insufficient to detect those coming from within it. In other words, low spiking is a good indicator for deeming that the recording is not from the STN. Still, a high spiking rate occurring outside of the STN is not uncommon and produces false positives as shown in the previous section.

Those false positives cause the sensitivity to be so unacceptably low.
In the case of all the attributes, the classifiers gave the following statistics:

Weka's Random Forest 10 fold cross validation:

Sensitivity:	0.933	Specificity:	0.988
Accuracy:	0.976	Coverage:	1.000

RSES 10- fold cross validation:

Sensitivity:	0.939	Specificity:	0.975
Accuracy:	0.967	Coverage:	1.000

When all the attributes are considered, both the sensitivity and specificity are very good. The sensitivity is ~0.93 and what is also very important, the specificity is very high ~0.99, which is extremely important as it minimizes the probability of labelling a non-STN region as STN.
The results of the classification are presented as a set of pictures similar to those presented in this paper and also in the form of a table. Table 1 shows the results of classification for pass of the electrodes used in previous examples in this paper.
'S' denotes recordings classified as ones coming from the STN. The grey background denotes the tip of the stimulating electrode as implanted during surgery.

Table I. Classification Results
Tabela I. Wyniki klasyfikacji

Electrode	-10000	-9000	-8000	-7000	-6000	-5000	-4000	-3000	-2000	-1000	0	1000	2000	3000	4000	5000
Anterior	M	M	M	M	M	M	M	M	**S**	**S**	**S**	**S**	**S**	M	M	M
Medial	M	M	M	M	M	M	M	M	**S**	**S**	**S**	**S**	**S**	M	M	M
Central	M	M	M	M	M	M	M	M	M	M	M	**S**	**S**	M	M	M

CONCLUSIONS

1. Cross validation tests have proven that the chosen attributes are sufficient enough for successful discrimination between recordings made within the STN and outside of it.
2. The software application that implements the attributes calculation process and presents the classification results has since the fall of 2013 been successfully used during PD DBS surgeries performed in the Institute of Psychiatry and Neurology in Warsaw.

APPENDIX

In this section, some more detailed technical information regarding microelectrode signal analysis is provided. The raw signal contains various contaminations, they are of different nature, and some of them are low frequency components while others are of an artifact nature. Spike detection can be facilitated in at least two ways i.e. based on their slope or their amplitude. Detection based upon slope focuses on the results provided by the first derivative of the signal. It is, however, difficult to automatically set the threshold which must be exceeded by the derivative to suspect that a spike might have occurred. That is why in this approach we selected the detection method that is amplitude based. It is assumed that if the amplitude exceeds 4 σ, then the necessary condition of spike occurrence is met. The difficulty lies in fact that the high amplitude of the spikes adversely influences the standard deviation i.e. when it is calculated in a standard way.

To overcome this difficulty, the standard deviation is estimated as

$$\sigma = \frac{median(|x_1|, \ldots, |x_n|)}{0.6745}$$

where x_1, … x_n are samples of the recording. This estimation has been defined in [9]. Furthermore, to achieve a successful amplitude spike detection, the signal has to be free of low frequency fluctuations. For this purpose, prior to spike detection, the signal is high pass filtered in order to remove frequencies below 187.5 Hz. To obtain less distorted spike shapes, some filtering is also done in frequencies above 6 Hz. For filtering purposes, the Discrete Wavelet Transform (DWT) has been used throughout this paper [21,22]. For the DWT the D4 Daubechies wavelet function has been used. DWT allows one to see a signal in various frequency bands. This is the core of the spike sorting and artifact removal processes. The Full Discrete Wavelet Transform also provides wavelet coefficients that are used to calculate the signal power in LFB and HFB attributes [23].
The software application implementing the described decision support system provides classification results after about two minutes of calculation. That makes it feasible to be used during surgery in the operation theatre.

ACKNOWLEDGEMENTS

This work was supported by DEC-2011/03/B/ST6/ 03816 from the Polish National Science Centre.

REFERENCES

1. Israel Z., Burchiel K.J. Microelectrode Recording in Movement Disorder Surgery. Thieme Medical Publishers 2004.
2. Nolte J. The Human Brain. An Introduction to Its Functional Anatomy. Elsevier 2009.
3. Defer G.L., Widner H., Marié R.M., Rémy P., Levivier M. Core assessment program for surgical interventional therapies in Parkinson's disease. Mov. Dis. 1999; 14: 572–584,.
4. Mallet L., Upbach M.S., N'Diaye K. et al. Stimulation of subterritories of the subthalamic nucleus reveals its role in the integration of the emotional and motor aspects of behavior. Proc. Nat. Acad. Sci. USA 2007; 104: 10661–10666.
5. Shapira N.A., Okun M.S., Wint D. et al. Panic and fear induced by deep brain stimulation. J. Neurol. Neurosurg.Psychiatry 2006; 77: 410–412.
6. Pizzolato G., Mandat T. Deep Brain Stimulation for Movement Disorders. Front. Integr. Neurosci. 2012; 6: 2. doi: 10.3389/fnint.2012.00002. eCollection 2012.
7. Mandat T., Tykocki T., Koziara H. et. al. Subthalamic deep brain stimulation for the treatment of Parkinson disease. Neurol. Neurochir. Pol. 2011; 45: 32–36.
8. Novak P., Przybyszewski A.W., Barborica A., Ravin P., Margolin L., Pilitsis J. Localization of the subthalamic nucleus in Parkinson disease using multiunit activity. J. Neurol. Sci. 2011; 310: 44–49.
9. Donoho D.L. De-Noising by Soft-Thresholding. IEEE Transactions On Information Theory 1995; 4(3): 613–627.
10. Quiroga R.Q., Nadasdy Z., Ben-Shaul Y. Unsupervised Spike Detection and Sorting with Wavelets and Superparamagnetic Clustering. Neural Comput. 2004; 16: 1661–1687.
11. Archer C., Hochstenbach M.E., Hoede C. et al. Neural spike sorting with spatio-temporal features. In: Proceedings of the 63rd European Study Group Mathematics with Industry, 28 Jan–1 Feb 2008, Enschede, The Netherlands, pp. 21–45.
12. Szlufik S., Koziorowski D., Ciecierski K. et al. DBS decision support system based on analysis of microelectrode recorded signals. Mov. Dis. 2012, 27, Abstract Suppl.: 168–169.
13. Ciecierski K., Raś Z., Przybyszewski A.W. Selection of the optimal microelectrode during DBS surgery in Parkinson's patients. Lecture Notes in Computer Science 2011; 6803: 554–564.
14. Pettersen K.H., Einevoll G.T. Amplitude variability and extracellular low-pass filtering of neuronal spikes. Biophys. J. 2008; 94: 784–802.
15. Zaidel A., Spivak A., Shpigelman L., Bergman H., Israel Z. Delimiting Subterritories of the Human Subthalamic Nucleus by Means of Microelectrode Recordings and a Hidden Markov Model. Mov. Dis. 2009; 24: 1785––1793.
16. Ciecierski K., Raś Z., Przybyszewski A.W. Foundations of automatic system for intrasurgical localization of subthalamic nucleus in Parkinson patients. Web Intelligence and Agent Systems 2014; 12: 63–82,.
17. Ciecierski K., Raś Z., Przybyszewski A.W. Foundations of Recommender System for STN Localization during DBS Surgery in Parkinson's Patients.

In: Foundations of Intelligent Systems. Eds. L. Chen, A. Felfernig, J. Liu, Z.W. Raś. Springer Verlag, Berlin 2012, pp. 234–243.
18. Ciecierski K., Raś Z., Przybyszewski A.W. Discrimination of the Micro Electrode Recordings for STN Localization during DBS Surgery in Parkinson's Patients. In: Flexible Query Answering Systems. Eds. H.L. Larsen, M.J. Martin-Bautista, M. Amparo Vila, T. Andreasen, H. Christiansen. Springer Verlag, Berlin 2013, pp. 328–339.
19. Pawlak Z. Rough Sets: Theoretical Aspects of Reasoning About Data. Kluwer Academic Publishers, Dordrecht 1991.
20. Bazan J., Szczuka M. RSES and RSESlib – A Collection of Tools for Rough Set. In. Lecture Notes in Artificial Intelligence, Springer Verlag, 2005, pp. 106–113.
21. Wiltschko A.B., Gage G.J., Berke J.D. Wavelet Filtering before Spike Detection Preserves Waveform Shape and Enhances Single-Unit Discrimination. J. Neurosci. Methods 2008; 173: 34–40.
22. Jensen A., Ia Cour-Harbo A. Ripples in Mathematics. Springer Verlag 2001.
23. S. W. Smith. Digital Signal Processing. Elsevier 2003.